Design of unobscured reflective zoom system with three mirrors

Tingcheng Zhang (张庭成), Yongtian Wang (王涌天)*, and Jun Chang (常 军)

Laboratory of Optoelectronic Technology and Information System, Beijing Institute of Technology, Beijing 100081, China

**E-mail: wyt@bit.edu.cn*

Received February 26, 2010

A method for the design of an unobscured reflective zoom system with three mirrors is described. This method applies the vector aberration theory, which helps designers analyze third-order aberrations for optical systems with decentered and tilted surfaces. As the vector aberration theory presents the variation of third-order aberrations in asymmetric systems through analytic expressions, real ray tracing is unnecessary. Hence, the design with vector aberration theory is faster, and the analytic expressions are more comprehensive and intuitive. To demonstrate the practicability of the method, a design example is given, which shows that the presented method can guide designers achieve a good unobscured reflective zoom system with three mirrors.

OCIS codes: 220.4830, 220.1000, 220.1140, 110.6770.

doi: 10.3788/COL20100807.0701.

All reflective zoom systems have the advantages of low weight, high transmission, uniform performance over a broad spectral band[1], radiation resistance, and thermal stability compared with refractive zoom systems. However, the obscurations in traditional co-axial reflective systems have made the design of zoom systems with large field of view difficult, and in some cases, impossible to handle. In order to eliminate obscurations, decenters and tilts of the mirrors were incorporated into asymmetric system designs[2]. However, due to the lack of rotational symmetry, the classical theory of Seidel aberrations has become unsuitable for the design of such systems.

Buchroeder described a class of non-axially symmetric systems constructed from axially-symmetric components[3]. With the vector aberration mentioned in Ref. [4], final system aberration fields could be located and analyzed[5−8]. Later, Rogers made some further developments[9−11]. With the emergence of high-speed computers, real ray tracing has become very fast, accurate, and cheap. Users can now employ real rays to construct the merit function for design optimization. However, compared with real ray tracing, the vector aberration theory could provide for the relationships between decenters and tilts, and change third-order aberrations through analytic expressions; these could help greatly in the initial stage of the design[12]. In practice, the vector aberration theory has always been used to design off-axis reflective systems with fixed focal length. However, it is seldom used in the design of zoom reflective systems.

In this letter, we present the vector aberration theory applied in the design of an unobscured reflective zoom system with three mirrors. The process of correcting the coma and astigmatism of a system with decentered and tilted surfaces is shown by using the vector aberration theory. A design example is also given to show how one can achieve a good unobscured reflective zoom system with three mirrors.

For a centered system, the third-order aberration contribution from the jth surface can be written in polar form as[13]

$$\begin{aligned} W_j(H,\rho,\rho\cos\boldsymbol{\phi}) = {} & W_{040j}\rho^4 + W_{131j}H\rho^3\cos\phi \\ & + W_{222j}H^2\rho^2(\cos\phi)^2 + W_{220j}H^2\rho^2 \\ & + W_{311j}H^3\rho\cos\phi, \end{aligned} \tag{1}$$

where H is the field radius coordinate normalized by the image height in the centered system, ρ is the pupil radius coordinate normalized by the exit pupil radius, and ϕ is the pupil azimuth coordinate with respect to an arbitrarily chosen meridian plane.

To obtain the vector form, we changed the field radius coordinate and pupil radius coordinate to vectors, as shown in Fig. 1. In this case, $\boldsymbol{H}$ represents the position in the image field with H_x and H_y with its components along $\boldsymbol{x}$ and $\boldsymbol{y}$, respectively; $\boldsymbol{\rho}$ represents the pupil position with ρ_x and ρ_y with its components along $\boldsymbol{x}$ and $\boldsymbol{y}$, respectively.

The third-order aberration contribution from the jth surface in vector form is given by

$$\begin{aligned} W_j(\boldsymbol{H},\boldsymbol{\rho}) = {} & W_{040j}(\boldsymbol{\rho}\cdot\boldsymbol{\rho})^2 + W_{131j}(\boldsymbol{H}\cdot\boldsymbol{\rho})(\boldsymbol{\rho}\cdot\boldsymbol{\rho}) \\ & + W_{222j}(\boldsymbol{H}\cdot\boldsymbol{\rho})^2 + W_{220j}(\boldsymbol{H}\cdot\boldsymbol{H})(\boldsymbol{\rho}\cdot\boldsymbol{\rho}) \\ & + W_{311j}(\boldsymbol{H}\cdot\boldsymbol{H})(\boldsymbol{H}\cdot\boldsymbol{\rho}). \end{aligned} \tag{2}$$

In asymmetric systems, centers of wave-front aberration contributions from different surfaces do not coincide

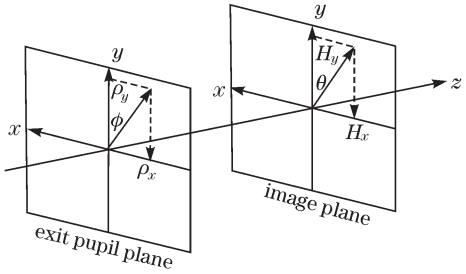

Fig. 1. Definition of $\boldsymbol{H}$ and $\boldsymbol{\rho}$.

at $\boldsymbol{H}=0$. They are displaced on the image plane. The displacement of the jth surface is denoted by a vector $\boldsymbol{\sigma}_j$, which is the projection of a line connecting the center of the pupil for the jth surface with the center of curvature of that surface to the image plane[5]. The pupil for the jth surface is the image of the entrance pupil formed by the optical surface numbers from 1 to $j-1$. The pupil for the first surface is the entrance pupil of the optical system. Thus, in asymmetric systems, the third-order aberration contribution from the jth surface becomes[14]

$$\begin{aligned}W_j(\boldsymbol{H},\boldsymbol{\rho}) = {} & W_{040j}(\boldsymbol{\rho}\cdot\boldsymbol{\rho})^2 + W_{131j}[(\boldsymbol{H}-\boldsymbol{\sigma}_j)\cdot\boldsymbol{\rho}](\boldsymbol{\rho}\cdot\boldsymbol{\rho}) \\ & + W_{222j}[(\boldsymbol{H}-\boldsymbol{\sigma}_j)\cdot\boldsymbol{\rho}]^2 \\ & + W_{220j}[(\boldsymbol{H}-\boldsymbol{\sigma}_j)\cdot(\boldsymbol{H}-\boldsymbol{\sigma}_j)](\boldsymbol{\rho}\cdot\boldsymbol{\rho}) \\ & + W_{311j}[(\boldsymbol{H}-\boldsymbol{\sigma}_j)\cdot(\boldsymbol{H}-\boldsymbol{\sigma}_j)] \\ & [(\boldsymbol{H}-\boldsymbol{\sigma}_j)\cdot\boldsymbol{\rho}]. \end{aligned} \tag{3}$$

The spherical aberration, which was unaffected by tilts or decenters since there was no dependence on field variable, could be written as

$$W_{\rm sph} = \sum_{j=1}^{m} W_{040j}(\boldsymbol{\rho}\cdot\boldsymbol{\rho})^2. \tag{4}$$

The coma was defined as

$$\begin{aligned}W_{\rm Coma} &= \sum_{j=1}^{m} W_{131j}[(\boldsymbol{H}-\boldsymbol{\sigma}_j)\cdot\boldsymbol{\rho}](\boldsymbol{\rho}\cdot\boldsymbol{\rho}) \\ &= \left[\left(\sum_{j=1}^{m} W_{131j}\boldsymbol{H} - \sum_{j=1}^{m} W_{131j}\boldsymbol{\sigma}_j\right)\cdot\boldsymbol{\rho}\right](\boldsymbol{\rho}\cdot\boldsymbol{\rho}). \end{aligned} \tag{5}$$

We let $\sum\limits_{j=1}^{m} W_{131j} = W_{131}$. When $W_{131}\neq 0$, Eq. (5) was rewritten as

$$\begin{aligned}W_{\rm Coma} &= W_{131}\left[\left(\boldsymbol{H} - \frac{\sum\limits_{j=1}^{m} W_{131j}\boldsymbol{\sigma}_j}{W_{131}}\right)\cdot\boldsymbol{\rho}\right](\boldsymbol{\rho}\cdot\boldsymbol{\rho}) \\ &= W_{131}[(\boldsymbol{H}-\boldsymbol{a}_{131}\cdot\boldsymbol{\rho}](\boldsymbol{\rho}\cdot\boldsymbol{\rho}), \end{aligned} \tag{6}$$

$$\boldsymbol{a}_{131} = \frac{\sum\limits_{j=1}^{m} W_{131j}\boldsymbol{\sigma}_j}{W_{131}}. \tag{7}$$

Based on Eq. (6), in asymmetric systems, the center of third-order coma was changed from $\boldsymbol{H}=0$. It was decided by the vector $\boldsymbol{a}_{131}$.

Based on Eq. (1) and having recognized that the term for the medial astigmatic component was $W_{220\rm M} = W_{220} + \frac{1}{2}W_{222}$, we obtained:

$$\begin{aligned}W_{\rm Ast} + W_{\rm Cur} &= \sum_{j=1}^{m} W_{222j}H^2\rho^2(\cos\phi)^2 + \sum_{j=1}^{m} W_{220j}H^2\rho^2 \\ &= \frac{1}{2}\sum_{j=1}^{m} W_{222j}H^2\rho^2\cos(2\phi) \\ &\quad + \sum_{j=1}^{m} W_{220{\rm M}j}H^2\rho^2. \end{aligned} \tag{8}$$

Using "vector multiplication"[5], $\boldsymbol{A}^2 = [a\exp(\mathrm{i}\alpha)]^2 = a^2\exp(\mathrm{i}2\alpha)$, Eq. (8) was rewritten in a vector form as

$$\begin{aligned}W_{\rm Ast} + W_{\rm Cur} = {} & \frac{1}{2}\sum_{j=1}^{m} W_{222j}\boldsymbol{H}^2\boldsymbol{\rho}^2 \\ & + \sum_{j=1}^{m} W_{220{\rm M}j}(\boldsymbol{H}\cdot\boldsymbol{H})^2(\boldsymbol{\rho}\cdot\boldsymbol{\rho})^2. \end{aligned} \tag{9}$$

By substituting $\boldsymbol{H}-\boldsymbol{\sigma}_j$ for $\boldsymbol{H}$, Eq. (9) was further transformed into

$$\begin{aligned}W_{\rm Ast} + W_{\rm Cur} = {} & \frac{1}{2}\sum_{j=1}^{m} W_{222j}(\boldsymbol{H}-\boldsymbol{\sigma}_j)^2\cdot\boldsymbol{\rho}^2 \\ & + \sum_{j=1}^{m} W_{220{\rm M}j}[(\boldsymbol{H}-\boldsymbol{\sigma}_j)\cdot(\boldsymbol{H}-\boldsymbol{\sigma}_j)]^2 \\ & (\boldsymbol{\rho}\cdot\boldsymbol{\rho})^2. \end{aligned} \tag{10}$$

The first term in Eq. (10) denotes astigmatism while the second term denotes the average field curvature. Similar to the coma, after the rearrangement of the first term, we obtained

$$W_{\rm Ast} = \frac{1}{2}W_{222}[(\boldsymbol{H}-\boldsymbol{a}_{222})^2 + \boldsymbol{b}_{222}^2]\cdot\boldsymbol{\rho}^2, W_{222}\neq 0, \tag{11}$$

where

$$\boldsymbol{a}_{222} = \frac{\sum\limits_{j=1}^{m} W_{222j}\boldsymbol{\sigma}_j}{W_{222}},\ \boldsymbol{b}_{222} = \frac{\sum\limits_{j=1}^{m} W_{222j}\boldsymbol{\sigma}_j^2}{W_{222}} - \boldsymbol{a}_{222}. \tag{12}$$

The center of the astigmatism was then decided by

$$\begin{aligned}\boldsymbol{H} &= \boldsymbol{a}_{222} \pm \mathrm{i}\boldsymbol{b}_{222},\ \text{where}\ \pm\mathrm{i}\boldsymbol{b}_{222} = \pm\mathrm{i}(\boldsymbol{b}_{222}\mathrm{e}^{\mathrm{i}\beta}) \\ &= \boldsymbol{b}_{222}\mathrm{e}^{\mathrm{i}(\beta\pm\pi/2)}. \end{aligned} \tag{13}$$

Based on Eq. (13), there were generally two zeros or nodes for astigmatism in asymmetric systems. The symmetric system is merely a special case.

The displacement vector $\boldsymbol{\sigma}_j$ is a function of the equivalent tilt $\boldsymbol{\beta}_{0j}$, which can be expressed as

$$\boldsymbol{\beta}_{0j} = \boldsymbol{\beta}_j + c_j\delta\boldsymbol{v}_j = c_j\delta\boldsymbol{c}_j, \tag{14}$$

where c_j is the curvature of the jth surface, $\boldsymbol{\beta}_j$ is the tilt of the jth surface, $\delta\boldsymbol{v}_j$ is the decenter of the jth surface, and $\delta\boldsymbol{c}_j$ is the displacement of the center of curvature of the jth surface. Owing to the variable optical characteristics of a zoom system, we denoted $\boldsymbol{a}_{131p}$ and $(\boldsymbol{a}_{222}\pm\mathrm{i}\boldsymbol{b}_{222})_p$ as the centers of coma and astigmatism, respectively, for the pth configuration of the zoom system. Thus,

$$\begin{aligned}\boldsymbol{a}_{131p} = \boldsymbol{a}_{131p}[(\boldsymbol{\sigma}_j)_p] = \boldsymbol{a}_{131p}(\boldsymbol{\beta}_j,\delta\boldsymbol{v}_j), \\ j=1,\cdots,m, \end{aligned} \tag{15}$$

$$\begin{aligned}(\boldsymbol{a}_{222}\pm\mathrm{i}\boldsymbol{b}_{222})_p &= \boldsymbol{a}_{222p}[(\boldsymbol{\sigma}_j)_p] \pm \mathrm{i}\boldsymbol{b}_{222p}[(\boldsymbol{\sigma}_j)_p] \\ &= \boldsymbol{a}_{222p}(\boldsymbol{\beta}_j,\delta\boldsymbol{v}_j) \pm \mathrm{i}\boldsymbol{b}_{222p}(\boldsymbol{\beta}_j,\delta\boldsymbol{v}_j), \\ & j=1,\cdots,m, \end{aligned} \tag{16}$$

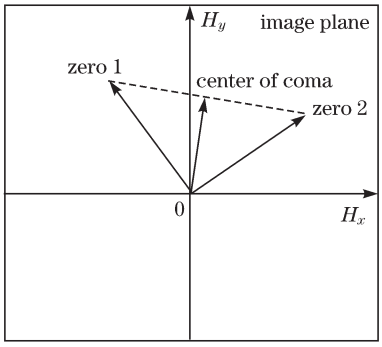

Fig. 2. Correction of coma and astigmatism.

To minimize wavefront aberration, it was desirable for us to make the center of coma coincide with the center of the line connecting the two nodes of astigmatism for each configuration of the zoom system. We employed this by setting the initial decenter and tilt values of surfaces, i.e., $\boldsymbol{a}_{131p} = \boldsymbol{a}_{222p}$ (Fig. 2).

From the abovementioned discussion, it is clear that the initial layout of an unobscured reflective zoom system could be obtained by solving

$$\boldsymbol{a}_{131p}(\boldsymbol{\beta}_j, \delta\boldsymbol{v}_j) - \boldsymbol{a}_{222p}(\boldsymbol{\beta}_j, \delta\boldsymbol{v}_j) = 0, \quad j = 1, \cdots, m,\ p = 1, \cdots, n, \tag{17}$$

on the condition that all of the obscurations are eliminated. We could then decide on the decenters and tilts for all surfaces. Coma and astigmatism could also be corrected.

The vector aberration theory was applied to design an unobscured reflective zoom system with three mirrors. This system had a zoom ratio of 4:1. Its entrance pupil diameter was 37.5 mm, and $F/\#$ range was from 4 to 12. A centered reflective zoom system is shown in Table 1. However, this system was found unsuitable for application due to its unacceptable obscurations. We eliminated these obscurations by introducing decenters and tilts to the mirrors under the premise of correcting errors in coma and astigmatism.

Table 1. Parameters of Centered Reflective Zoom System

Surface	Radius (mm)	Conic Coefficient	Separation (mm)
Stop	Infinity	0	200
Primary	−340.212	−0.926	
Secondary	−81.715	−7.365	−175.640, −156.511, −148.1619
Tertiary	−203.695	−0.029	198.693, 208.774, 211.626
Image	Infinity	0	−208.482, −227.085, −262.881

Equivalent tilts, $\boldsymbol{\beta}_{0j}$ ($\boldsymbol{\beta}_j$, $\delta\boldsymbol{v}_j$), j=1, 2, 3, were introduced to the mirrors. They became scalar because the mirrors were decentered in the Y direction and tilted around the X axis. To avoid obscurations, a set of equations and constraints were identified based on Eq. (17):

$$\begin{cases} \boldsymbol{a}_{131,1}(\boldsymbol{\beta}_j, \delta\boldsymbol{v}_j) = \boldsymbol{a}_{222,1}(\boldsymbol{\beta}_j, \delta\boldsymbol{v}_j) \\ \boldsymbol{a}_{131,2}(\boldsymbol{\beta}_j, \delta\boldsymbol{v}_j) = \boldsymbol{a}_{222,2}(\boldsymbol{\beta}_j, \delta\boldsymbol{v}_j), \quad j = 1, 2, 3, \\ \boldsymbol{a}_{131,3}(\boldsymbol{\beta}_j, \delta\boldsymbol{v}_j) = \boldsymbol{a}_{222,3}(\boldsymbol{\beta}_j, \delta\boldsymbol{v}_j) \end{cases} \tag{18}$$

$$\begin{cases} \boldsymbol{\beta}_1 + c_1\delta\boldsymbol{v}_1 > 0.122 \\ \boldsymbol{\beta}_2 + c_2\delta\boldsymbol{v}_2 > 0 \\ \boldsymbol{\beta}_3 + c_3\delta\boldsymbol{v}_3 < 0.297 \end{cases} \tag{19}$$

The values on the right side of the expression (19) are the equivalent tilts at which no ray was obscured. For example, by decentering the primary mirror by 13.84 mm in the $-Y$ direction and tilting it around the X axis by 4.66° clockwise, we could eliminate the obscuration of the primary mirror by the secondary mirror. By substituting these values into Eq. (14), a minimum value of 0.122 was obtained (see expression (19)).

By solving Eq. (18) and expression (19), a set of initial values for the decenters and tilts of the mirrors were obtained (Table 2). These eliminated the obscuration in the system (Fig. 3). The third-order coma and astigmatism of the system were also corrected.

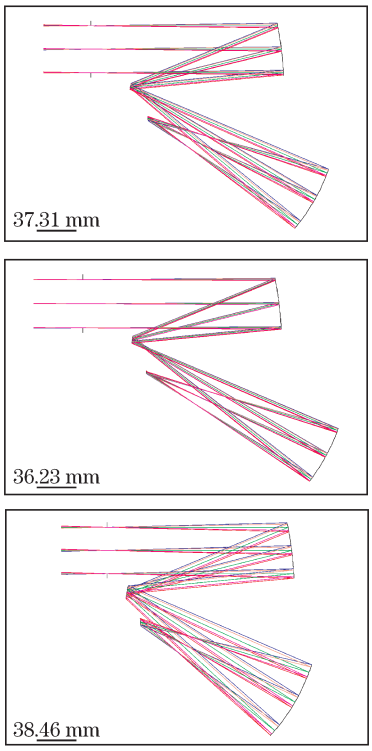

Fig. 3. Reflective zoom system with three mirrors after introducing initial decenter and tilt values.

Table 2. Decenters and Tilts of Mirrors

Mirror	Decenter (mm)	Tilt (deg.)
Primary	1.168	7.196
Secondary	−6.045	12.761
Tertiary	4.004	24.126

After simple optimization, a new unobscured reflective zoom system was achieved. Tables 3 and 4 give the construction parameters of the system, and Fig. 4 shows the modulation transfer function (MTF) curves for different zoom positions. From the MTF curves, we see that the zoom system manifests diffraction-limited image quality. The changes of the equivalent tilts during the optimization were 0.0882 and −0.4421 for the primary and secondary mirrors, respectively. The values are very small.

Table 3. Parameters of Unobscured System

Mirror	Radius (mm)	Aspherical Coefficients: Conic, 4th, 6th, 8th, and 10th order coefficient	Separation (mm)
Stop	Infinity	0,0,0,0,0	500
Primary	−335.191	$-1.132, 7.138\times10^{-10}, -8.780\times10^{-13}, 1.322\times10^{-16}, -8.790\times10^{-21}$	−170.511, −161.685, −157.878,
Secondary	−29.7622	$-7.405, 2.697\times10^{-7}, -7.587\times10^{-13}, -3.492\times10^{-15}, 2.078\times10^{-19}$	195.335, 206.812, 212.546,
Tertiary	−204.497	$-0.035, 4.647\times10^{-11}, -2.111\times10^{-15}, -4.345\times10^{-20}, 6.736\times10^{-24}$	−195.356, −205.164, −218.321,
Image	Infinity	0,0,0,0,0	

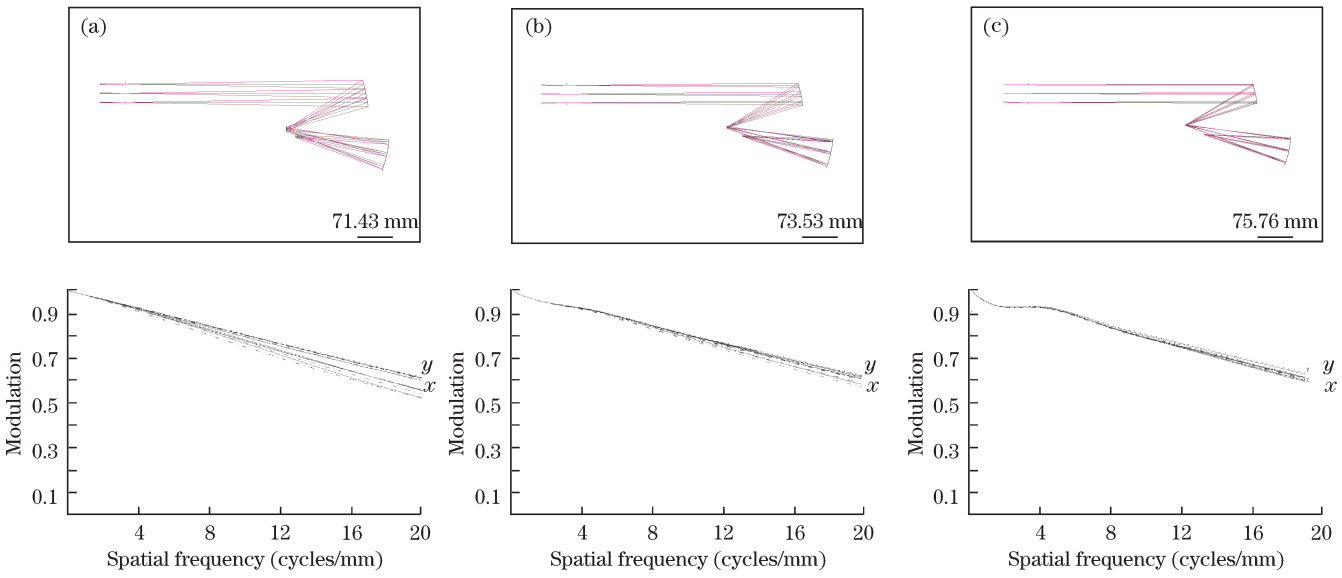

Fig. 4. Layout and MTF for the zoom position with (a) wide field of view, (b) middle field of view, and (c) narrow field of view.

Table 4. Decenters and Tilts of Mirrors after Optimization

Mirror	Decenter (mm)	Tilt (deg.)
Primary	−33.473	6.331
Secondary	11.780	14.345
Tertiary	4.004	24.126

In conclusion, we present a simple and practicable method for the design of unobscured reflective zoom systems with three mirrors. By solving a set of equations under the guidance of the vector aberration, this method allows for the designation of a set of proper decenters and tilts for the mirrors. These can remove obscurations in the zoom system, and can correct coma and astigmatism at the same time. The method is very quick and straightforward. The system with the introduced decenters and tilts can serve as a new starting point for further optimization of the system.

References

1. H. Ma, X. Zhang, X. He, and Z. Nie, Acta Opt. Sin. (in Chinese) **29,** 3503 (2009).
2. M. Liang, N. Liao, J. Feng, Y. Lin, and D. Cui, Acta Opt. Sin. (in Chinese) **28,** 1359 (2008).
3. R. A. Buchroeder, "Tilted component optical systems", PhD Thesis (University of Arizona, 1976).
4. R. V. Shack and K. Thompson, Proc. SPIE **251,** 149 (1980).

5. K. Thompson, "Aberration fields in tilted and decentered optical systems", PhD. Thesis (University of Arizona, 1980).
6. K. Thompson, Proc. SPIE **2774,** 2 (1996).
7. K. Thompson, J. Opt. Soc. Am. A **22,** 1389 (2005).
8. K. Thompson, Proc. SPIE **27,** 127 (1980).
9. J. R. Rogers, Proc. SPIE **554,** 76 (1985).
10. J. R. Rogers, Opt. Eng. **39,** 1776 (2000).
11. J. R. Rogers, Proc. SPIE **3737,** 286 (1999).
12. X. Yang, Z. Wang, G. Mu, and F. Lian, Acta Photon Sin, (in Chinese) **34,** 1658 (2005).
13. J. M. Geary, *Introduction to Lens Design with Practical Zemax Examples* (Willmann-Bell, California, 2002).
14. T. S. Turner, Jr., Proc. SPIE **1752,** 184 (1992).